Sigma J Eng & Nat Sci 38 (4), 2020, 1999-2011

Sigma Journal of Engineering and Natural Sciences
Sigma Mühendislik ve Fen Bilimleri Dergisi

Research Article

AN EXPERIMENTAL APPROACH FOR FRICTION STIR WELDING: A CASE STUDY FOR AA 2024 – T351

Şefika KASMAN*[1], Sertan OZAN[2]

[1]*Dokuz Eylul University, Department of Mechanical Engineering, IZMIR;* ORCID: 0000-0002-4722-9203
[2]*Yozgat Bozok University, Department of Mechanical Engineering, YOZGAT;* ORCID: 0000-0003-1932-8308

Received: 07.04.2020 Revised: 22.09.2020 Accepted: 23.10.2020

ABSTRACT

In this study, AA 2024-T351 aluminum alloy plates were butt-welded using friction stir welding process at a constant welding speed of 63 mm/min and tool rotational speed of 400 and 630 rpm. Two welding seams were overlapped via shifting the pin towards advancing side or retreating side. The effect of friction stir welding parameters on mechanical and microstructural properties were investigated. Microstructural investigations and micro-hardness measurements were performed on the transverse cross section of welded joints. The decrease in tensile strength is attributed to the increase in tool rotational speed, leading to an increase in frictional heat generation regardless of overlapping of weld seams. Consistent correlation between tool pin type and other process parameters was found to occur, revealing that the higher tensile strength values were obtained in case pentagonal shaped pin was used. It was revealed that tapered threaded pin profile was resulted in producing defective welded joints; defects, located in the stir zone, were found to be effective on deteriorating the mechanical properties of welded joints.
Keywords: Friction stir welding, overlapping of weld seams, mechanical properties, microstructure, AA 2024 – T351.

1. INTRODUCTION

Aluminum alloys are functional materials used in automotive, aircraft, shipbuilding and transportation industries [1]. The welding applications in those industries require special care; it is worth noting that some of the materials are accepted to be welded problematically using conventional fusion welding techniques. Even 2XXX and 7XXX series of aluminum alloys are accepted to be the most popular alloys in the relevant industries namely automotive and aircraft, the welding procedure of those alloys is well-known to be welded problematically using fusion welding techniques [2-6] due to the tendency of formation of defects; e.g. hot cracking [2, 4, 6], solidification defects, porosity [4, 6] and hydrogen solubility [7]. Those defects are located in the fusion zone originating from melting and subsequent fast solidification, thus deteriorating the mechanical strength of the welded joints. The defects, observed in fusion welding processes, could be eliminated using the friction stir welding (FSW) technique. FSW technique is one of the solid-state welding techniques in which no melting and re-solidification of a metal occurs during and following the welding process. The most important characteristic feature of the FSW

* Corresponding Author: e-mail: sefika.kasman@deu.edu.tr, tel: (232) 301 92 17

technique is the formation of plastic deformation, originating from the movement of a rotary tool with the high frictional heat. A sufficient amount of plastic deformation and heat input provide an effective bonding between the two plates to be welded. While the rotating tool governs the intensity of frictional heat and plastic deformation; notably, heat input per unit area is determined by the welding speed (WS). The tool, used in a FSW process, is consisted of two characteristic parts, namely pin and shoulder. With the rotation of the tool, the spinning pin is pressed against the abutted surface of the plates to be welded, relocating the plasticized material from the advancing side (AS) towards the retreating side (RS) along the weld line [7]. Thus, a weld joint is formed by the rotating tool which moves along the weld line. It is worth noting that, such a solid phase bonding between the two plates to be joined makes the FSW process popular among the welding techniques preferred in the joining processes of aluminum alloys [8].

AA 2024 aluminum alloy is a widely used alloy in aircraft structures [9-13]; it exhibits superior corrosion resistance, relatively high mechanical strength [10-12] and fatigue strength [12, 13]. In this study, AA 2024-T351 alloy plates were subjected to a special FSW technique in order to improve tensile properties. The overlapping phenomenon of weld seams is the characteristic feature of this special FSW technique. In this study, the effects of overlapping phenomenon on the mechanical properties of welded joints, produced via pin offset technique, were investigated by taking FSW parameters and pin offset direction into consideration.

The overlapping process of weld seams is performed via offsetting the pin with a pre-determined distance towards the AS or RS following the obtainment of the first weld seam. Welded joints, produced using this technique, are accepted to be distinctly different from the welded joints consisting of single FS weld seam. The schematic illustration of a welded joint, produced via pin offsetting is shown in Fig. 1. To the best of our knowledge, in the available and open literature, there is no study focusing on FSW process of AA 2024 using pin offset technique. Notably, researchers produced overlapped weld seams in the joining process of AA 7075 [14-16], AA 6013 [17] and dissimilar alloys AA 6013/AA 7075 [18, 19]. This study aimed to provide a new approach to the FSW technique in order to improve the mechanical and microstructural properties of FS welded AA 2024-T351 aluminum alloy joints.

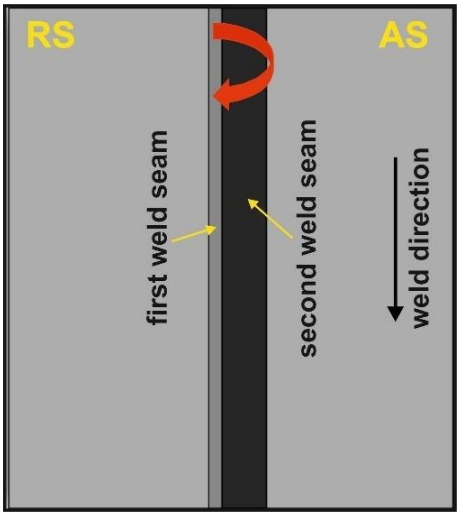

Figure 1. Schematic illustration of weld seam overlapping in a FSW process

2. EXPERIMENTAL PROCEDURES

AA 2024 – T351 plates, with a nominal composition of 3.91% Cu, 1.23% Mg, 0.52% Mn, 0.14% Fe and balance aluminum, were 225 mm in length, 100 mm in width and 6 mm in thickness. The abutting faces of the work-piece plates were machined in order to provide an effective contact, thereby preventing the separation with the effect of vertical force of tool pin. The welding processes were performed using universal milling machine. The work-piece plates were placed on a backing plate; support plates were subsequently positioned on the work-piece plates and clamped with studs as shown in Fig. 2a. The tool pin, used in the weld applications, were made of H13 hot-work tool steel. A tool for FSW is configured with pin shape. Two different pins, namely pentagonal (P) and tapered threaded (TT), were selected in the present study. The tool and pin configurations are given in Figs. 2b and c. The plunge depth for pin was fixed to be 5.90 mm. While the WS was fixed at 63 mm/min, the tool rotational speed (TRS) was set at two different rates, namely 400 and 630 rpm. The tool rotation axis is the normal to the rolling direction and it was tilted by 3°. The experiments were set at two different FSW conditions considering two different pin profiles. The FSW conditions are given in Table 1. All the FSW experiments were performed by considering the parameter's combinations given in Table 2.

Table 1. The FSW process parameters and their levels

Parameters (unit)	Symbol	Levels		
Tool pin type	TP	P		TT
Pin offset	PO	zero	2 mm-AS	2 mm-RS
Tool rotation speed (rpm)	TRS	400		630
Welding Speed (mm/min)	WS		63	

Microstructural observations were performed on the cross-section of the welded joints. The surface of the samples for microstructural observation and micro-hardness test were prepared according to the standard metallographic procedures; polished samples were subsequently etched using the Poulton's reagents. The microstructure of FS welded joints were observed using optical microscope. The micro-hardness measurements across the weld zone were performed with a load of 0.98 N and a dwell time of 15 s. The micro-hardness measurements were performed at 1 mm intervals. Tensile tests were performed with a cross-head speed of 2 mm/min in accordance with the ASTM E8/E8M [20]. The ultimate tensile strength and elongation at rupture of AA 2024-T351 is 456 MPa and 22 %, respectively. The grain size in the stir zone (SZ) was measured using the linear intercept method in accordance with the ASTM E112-13 [21]. In this study, the mechanical properties of FS welded joints were characterized using tensile strength and elongation at rupture (%) values. Three different test samples were prepared for each welding condition, and the average of the test results obtained from three different tests represented the average tensile strength and elongation at rupture (%) of the FS welded joint.

The mechanical properties of FS welded joints were analyzed using one-way ANOVA method. The Tukey HSD post hoc test revealed whether there was a significant difference between the groups and if $\rho < 0.05$, the differences between the samples were considered statistically significant.

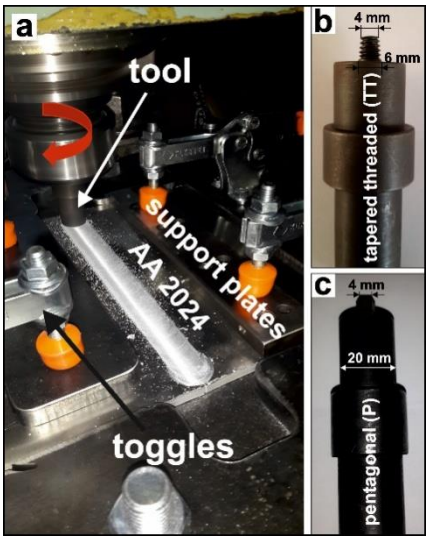

Figure 2. A sample FSW process and the tool pin profiles used in FSW applications

Table2. Experimental layout for FSW applications

Exp. No	Process Parameters			
	T	PO	TRS	WS
W1	P	0	400	63
W2	P	0	630	63
W3	P	AS	400	63
W4	P	AS	630	63
W5	P	RS	400	63
W6	P	RS	630	63
W7	TT	0	400	63
W8	TT	0	630	63
W9	TT	AS	400	63
W10	TT	AS	630	63
W11	TT	RS	400	63
W12	TT	RS	630	63

3. RESULTS AND DISCUSSION

3.1. Macro-structural Investigation of FSW Joints

The macro-structural observation was performed on the transverse cross-section of each welded joints. A detailed observation, given in Fig. 3, confirmed that all the welded joints were consisted of three distinct zones, namely SZ, thermo-mechanically affected zone (TMAZ) and heat affected zone (HAZ). The dark region, revealed as a consequence of etching process, was evaluated to be the base metal (BM). The confined intermediate region consisting of three different zones between two dark regions exhibited different shades as a consequence of etching. Moreover, the wideness of intermediate region exhibited differences. The main reason of the differences is attributed to the change in plastic deformation and the amount of frictional heat

input. The overlapping phenomenon of weld seams resulted in different regions, namely SZ-1 and SZ-2, in the SZ. Representative microstructures of SZ are shown in Fig. 4-W3, W5 and W6. While W3 was produced by overlapping two weld seams via shifting the pin towards AS, the W5 and W6 were produced via shifting the pin towards RS. This type of structure occurred in case two weld seams were overlapped, causing complex microstructure to occur. It was observed that an increase in TRS caused the wideness of weld zone consisting of SZ and TMAZ to increase. In addition to the effect of TRS on the width of the weld zone, shifting the pin towards AS or RS resulted in the weld zone to be expanded.

Macrostructure images exhibiting the regions marked with yellow arrows and circles in Fig. 4 at W7-W12 belong to defective joints; notably, cavity and tunnel-type defects were found to occur. The tunnel-type defect was encountered in joints welded with the TRS of 630 rpm using a tapered threaded pin profile. The defects were observed to be located at the root of weld seam. The tunnel type defects are occurred under the conditions of improper flow of the material and insufficient heat input as reported elsewhere [7].

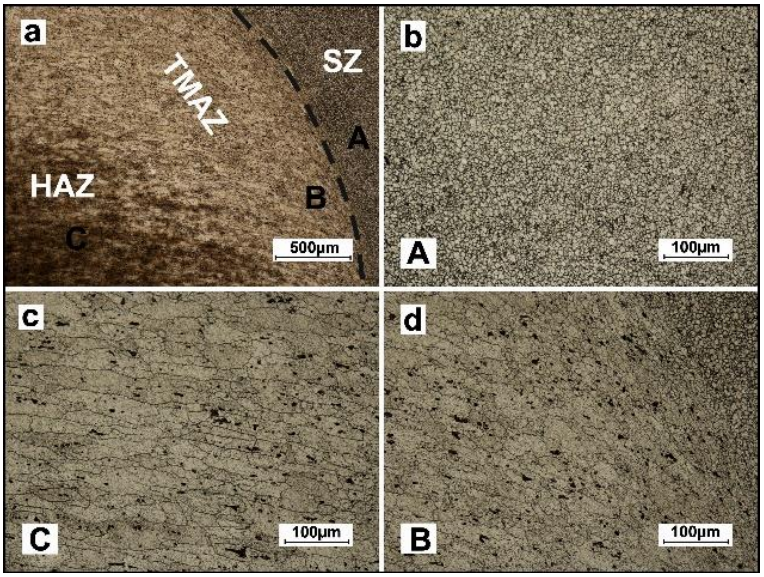

Figure 3. The transition zones for W1

The region, referred SZ, was located on the contact surface of BMs; it was exposed to common effect of the intense plastic deformation and frictional heat, causing changes to occur in the grain structure. Fig. 3a exhibits three distinct zones taken from W1. Fig. 3-A was obtained from the SZ and the grain size was found to be relatively finer and equiaxed in comparison to that of the TMAZ; the finer grain size is attributed to dynamical recrystallization process with the effect of intense plastic deformation and frictional heat. During the FSW process, the weld seam is under the effect of both extrusion and forging processes. It is considered that the downward force of a tool, TRS and WS determine the formation of those two above-mentioned processes and the capability of obtaining defect-free welded joints. The TMAZ is a region, located adjacent to the SZ; however, recrystallization does not occur in this region [3]. The effect of frictional heat is accepted not to be high enough to initiate a transformation on grain structure. This region is characterized by the grains which are oriented towards the direction of maximum shear stress [7]; it is worth noting that it exhibits finer grain size than that of the HAZ. This characteristic structure

is seen in Fig. 3a and Fig. 3a-B. A distinct border was found to occur between TMAZ and SZ as reported elsewhere [3]. Birol et. al. [7] reported that the distortion within the grains was revealed to be intensive between TMAZ and SZ and on the region, under tool shoulder, originating from the intensive effect of plastic deformation. It is worth noting that the stirring effect and frictional heat control the features of TMAZ.

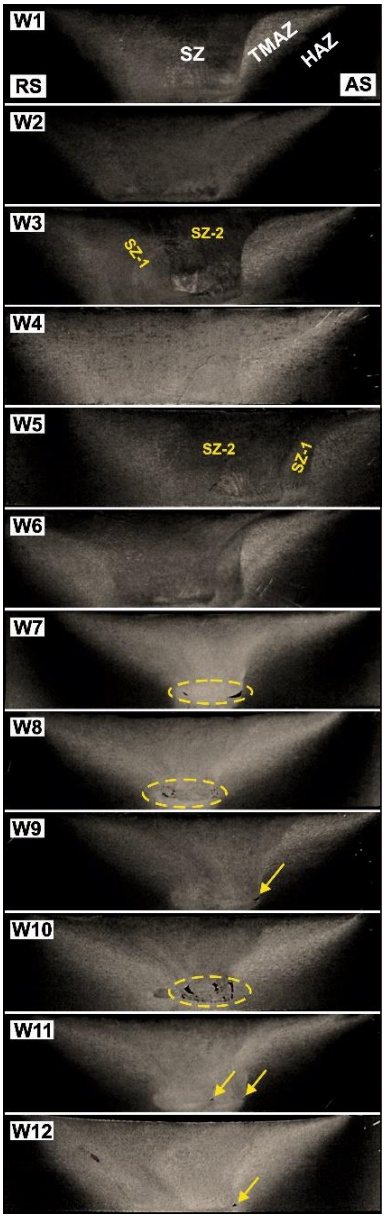

Figure 4. Macrostructure of FSW samples

3.2. Micro-structural Investigation of FSW Joints

The effect of intensive plastic deformation and cooling rate on the microstructural evolution of FS welded joints were investigated using optical microscopy. Fig. 5 exhibits the microstructural images of SZ; it was revealed that the microstructure was consisted of finer equiaxed grains in comparison to that of BM as reported elsewhere [3]. The SZ was revealed to be divided into three region which were under the shoulder (Fig. 5a), at the center of the SZ (Fig. 5b) and at the root of the SZ (Fig. 5c). The average grain size in Figs. 5a-c was measured to be 3.49 μm ± 0.35, 4.68 μm ± 0.34 and 2.92 μm ± 0.29, respectively. The average grain size in SZ of W1, W2, W3, W4, W5 and W6 was measured to be 4.68 ± 0.34 μm, 2.73 ± 0.26 μm, 4.77 ± 0.44 μm, 3.30 ± 0.50 μm, 4.04 ± 0.46 μm, 3.83 ± 0.32 μm. The grain size in the SZ of W1-W6 was evaluated to be related to the TRS; it was revealed that any increase in TRS caused the grain size to be finer as reported elsewhere [8, 22]. The overlapping phenomenon of weld seams is evaluated to be a complex process, creating a different deformation rate in SZ. This phenomenon may result in a differentiation on the grain size of SZ.

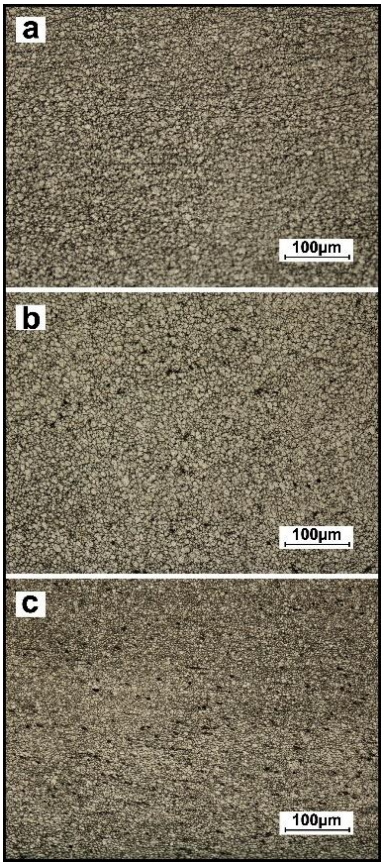

Figure 5. The change in the grain size for W1 (a: under the shoulder; b: center of the SZ; C: root of the SZ)

Small segments were found to occur as seen in Figs. 6b, b′, c′ and c″. While the magnified images of the segments in Figs. 6b and b′ are shown in Fig. 6b″, the other segments are shown in Figs. 6c′ and c″. It was revealed that those segments were consisted of precipitates; notably, they were located through a zig-zag line. The precipitates were found to be oriented towards the deformation way and tool rotation direction as seen in Figs. 6a and a′. The EDS results revealed that those precipitates could be $(Al,Cu)_xMn$, $Al(Cu,Fe,Mn)$, $(Al,Cu)_x(Fe,Mn)_ySi$ and Al_2CuMg as reported elsewhere [2, 4, 9, 23-25].

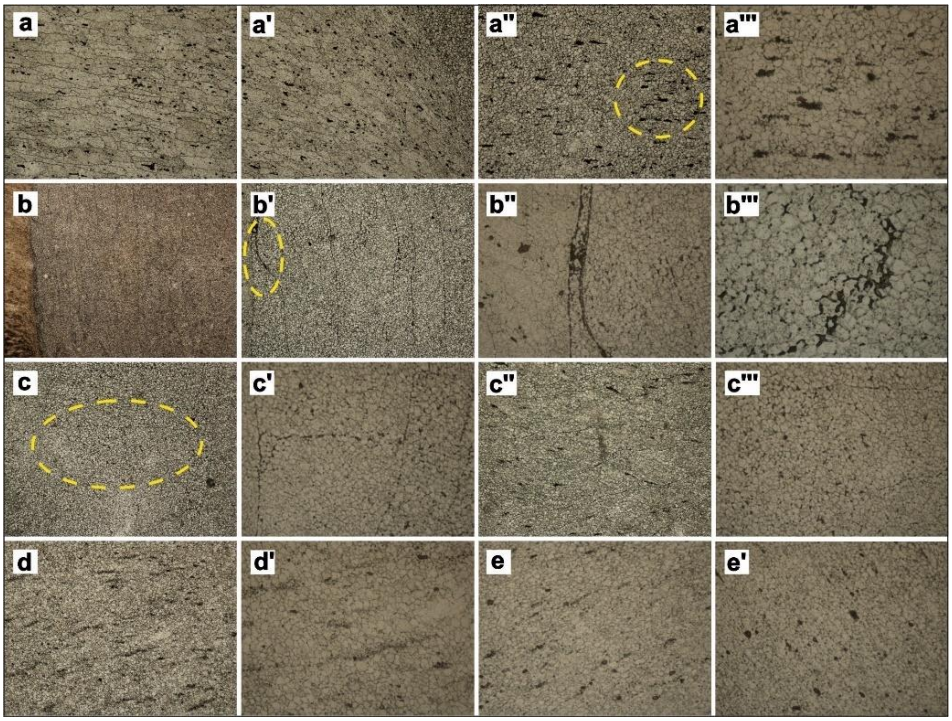

Figure 6. The segments shown in the SZ

3.3. Tensile properties of the FS welded joints

Tensile test results of FS welded joints are given in Fig. 7a and b. Experimental studies were performed under two groups considering the type of pin profile, namely pentagonal (Fig. 7a) and tapered threaded (Fig. 7b). The welding processes, performed on W1-6 samples, were carried out using a tool with pentagonal pin profile; however W7-12 joints were welded using a tool with tapered threaded pin profile. According to the tensile test results, the highest tensile strength and elongation at rupture (%) values were achieved using pentagonal pin profiled tool with the process parameters of 400 rpm TRS and 0 mm pin offset. In case the pin offset value was 0 mm, the increase in TRS value from 400 rpm to 630 rpm led to a decrease in tensile strength. Tensile strength values of W3 and W5 joints, joined with the process parameters of 400 rpm and 2 mm pin offset value, were measured to be 380 ± 8 and 379 ± 13 MPa, respectively. Notably, there was no significant difference ($\rho > 0.05$) between the tensile strength of W3 and W5. Increasing the TRS value from 400 rpm to 630 rpm for welded joints, produced using a pentagonal pin profiled tool, led to a decrease in tensile strength and elongation at rupture (%). When a sequence is made

in terms of tensile strength values of FS welded joints produced using a tool with pentagonal pin profile, it was revealed that FS welded joints are ranked W1 > W3 > W5 > W2 > W6 > W4. On the other hand, the elongation at rupture (%) of W1, W3 and W5 joints was measured to be 5.2%, 3.8% and 3.8%, respectively. W1, W3 and W5 joints, joined with the process parameter of 400 rpm TRS exhibited significantly higher ($\rho < 0.05$) elongation at rupture (%) value than W2, W4 and W6 joints welded with the process parameter of 630 rpm TRS. W9 joint exhibited the highest tensile strength with a value of 341 ± 22 MPa among the joints welded using a tool with tapered threaded pin profile. Notably, W9 joint was produced under the process parameters of 400 rpm TRS and 2 mm pin offset on the AS.

When a general evaluation is made; the increase of TRS from 400 rpm to 630 rpm for pentagonal and tapered threaded pin profiles, resulted in a decrease in tensile strength and elongation at rupture (%). It is worth noting that there was no significant differences ($\rho > 0.05$) between the tensile strength as well as elongation at rupture (%) of W7 and W8 welded joints. The geometry of the tool, used in the FSW process, was revealed to affect the mechanical properties of the joints. Tensile strength and elongation at rupture (%) of FS welded joints were measured to be in the range of 271-409 MPa and 0.4-5.2%, respectively. The lowest elongation at rupture (%) was obtained when using a tool with tapered threaded pin profile under the process parameters of 630 rpm TRS and 2 mm pin offset towards AS. Images showing the fracture location of the samples following the tensile test are given in Fig. 8. W1, 3, 5 and 6 joints, welded using pentagonal pin profiled tool, were observed to be fractured outside the SZ. W3 and W5 welded joints were observed to be fractured between HAZ and BM. This fracture location is quite close to the BM in the W5 joint, occurring on the AS of the welded joint. It was revealed that the fracture location was found to be between HAZ and TMAZ in W1 and W6 welded joints. Notably, the fracture location of W6 joint was observed to be closer to TMAZ. Fractures were observed to occur in the SZ of W2 and W4 joints. Notably, all welded joints, produced using a tapered threaded pin profiled tool, were detected to be fractured from the SZ.

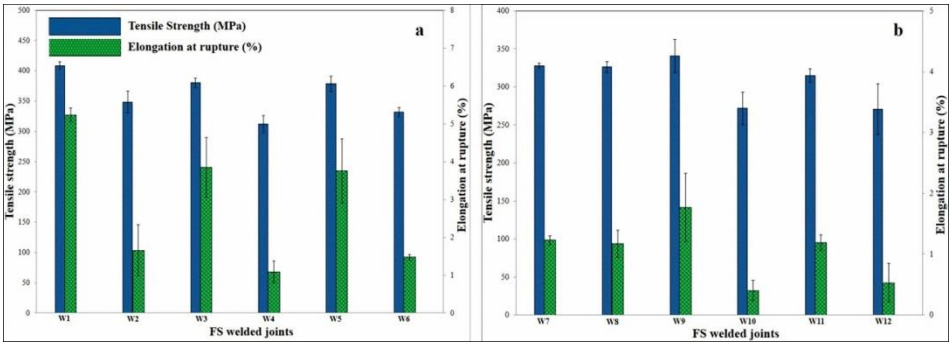

Figure 7. The change in the UTS and $\mathcal{E}_p$ according to the change in FSW condition

It is worth noting that a different type of pin profile, namely straight-helical has been used in our previous study [26].

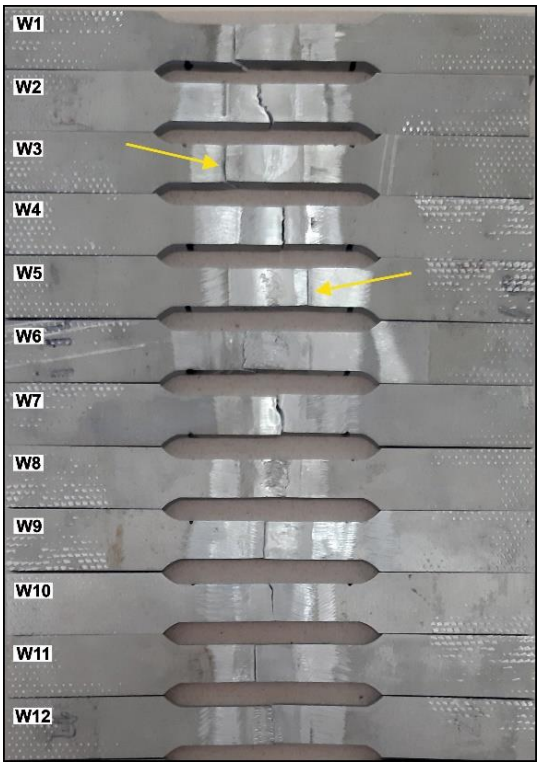

Figure 8. The fracture location of FS welded joints

3.4. Micro-Hardness Measurements

The change in hardness profile across the weld zone for each welded joint is seen in Fig. 9. The microstructural characteristics, mentioned above, were evaluated to be consistent with the micro-hardness measurements as reported elsewhere [25]. It was revealed that micro-hardness measurements of welded joints exhibited similar trend. The micro-hardness values increased gradually from BM to SZ. The highest micro-hardness was measured to be 155 HV in SZ of W1. The micro-hardness distributions in SZ of overlapped weld seams were revealed to be non-uniform originating from the higher deformation rate and different cooling behavior of weld zones as reported elsewhere [25]. It is considered that this non-uniformity is attributed to the overlapped weld seams, formation of second phase particles and precipitates [3]. The W10 joint was produced with the TRS of 630 rpm; however, the pin was offset towards AS following the formation of first weld seam. The micro-hardness values in overlapped region were measured to be in the range of 126-142 HV. The coarser grains are attributed to the overlapping effect, causing a decrease in micro-hardness values. Taking the differentiation in the micro-hardness into account, it was revealed that the micro-hardness values in SZ and TMAZ were high due to overlapped weld seams, intensive plastic deformation and heat input.

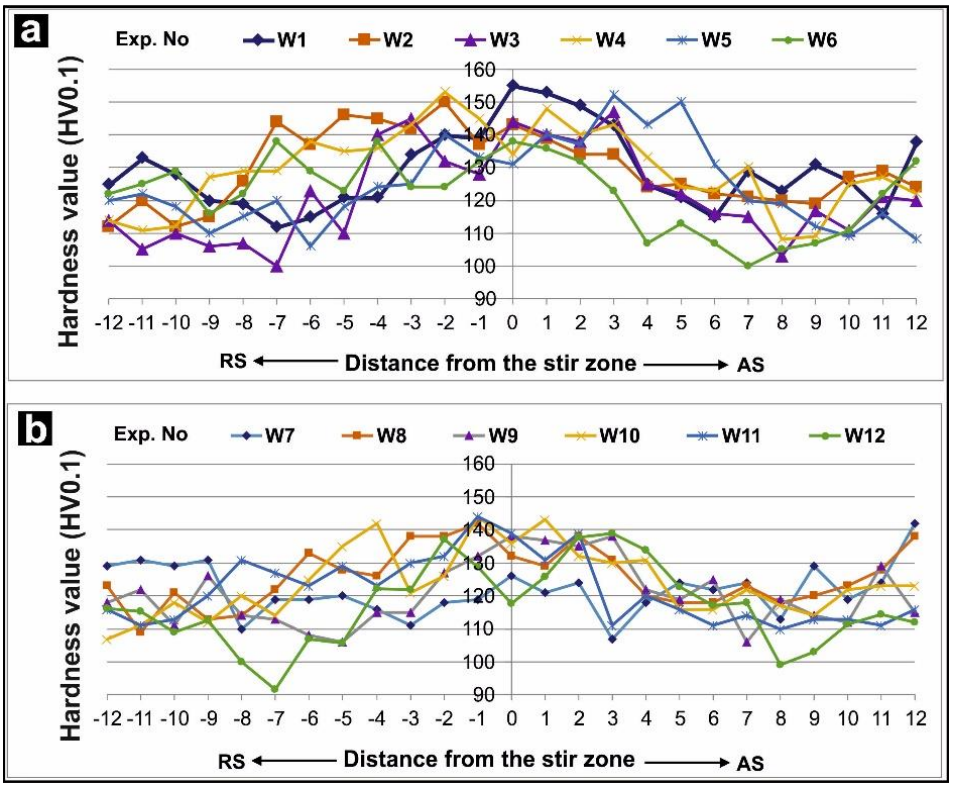

Figure 9. The change in hardness profile across the weld zone

4. CONCLUSIONS

In this study, pin overlap method was used in order to improve the mechanical properties of welded joints. TRS, tool pin profile were associated with weld seam overlap. According to the results obtained from the experiments, following conclusions were drawn;

a) The highest tensile strength and elongation at rupture (%) were obtained from the joint welded using pentagonal profiled pin with the process parameters of 400 rpm TRS and zero pin offset value. The tensile properties of the welded joints were deteriorated in case the TRS was increased from 400 rpm to 630 rpm.

b) The average grain size in SZ of a welded joint, produced using pentagonal profiled pin, was measured to be in the range of 2.73-4.77 µm. The increase in TRS caused the grain size in SZ to be finer. The coarsest grain size was measured in SZ of the welded joint which was produced with the process parameters of 400 rpm TRS and 2 mm pin offset value towards the AS.

c) The volumetric tunnel-type defect was observed in SZ of the welded joint produced using tapered threaded pin with the process parameters of 630 rpm TRS and 2 mm pin offset value towards the AS. Another defective weld seam, produced with tapered threaded pin, was found to be consisted of cavity-type defects. The cavity-type defect was found to be located on the AS and RS of welded joint produced with the process parameter of zero pin offset value.

Acknowledgement

The present study was supported by Dokuz Eylul University under project no. 2017.KB.FEN.002. The authors would like to acknowledge this financial support.

REFERENCES

[1] Boulahem, K., Ben Salem, S. and Bessrour, J. (2018) Prediction model of ultimate tensile strength and investigation on microstructural characterization of friction stir welded AA2024-T3,*The International Journal of Advanced Manufacturing Technology* 95(1), 1473-1486.

[2] do Vale, N. L., Torres, E. A., Santos, T. F. d. A., Urtiga Filho, S. L. and dos Santos, J. F. (2018) Effect of the energy input on the microstructure and mechanical behavior of AA2024-T351 joint produced by friction stir welding,*Journal of the Brazilian Society of Mechanical Sciences and Engineering* 40(9), 467-481.

[3] Khodir, S. A., Shibayanagi, T. and Naka, M. (2006) Microstructure and Mechanical Properties of Friction Stir Welded AA2024-T3 Aluminum Alloy,*Materials Transactions* 47(1), 185-193.

[4] Genevois, C., Deschamps, A., Denquin, A. and Doisneau-cottignies, B. (2005) Quantitative investigation of precipitation and mechanical behaviour for AA2024 friction stir welds,*Acta Materialia* 53(8), 2447-2458.

[5] Di, S., Yang, X., Luan, G. and Jian, B. (2006). Comparative study on fatigue properties between AA2024-T4 friction stir welds and base materials. *Materials Science and Engineering: A*, 435-436, 389-395.

[6] Leonard, A. and Lockyer, S. (2003). Flaws in friction stir welds. In: The proceedings of the 4th international conference on Friction Stir Welding, Park City, UT.

[7] Birol, Y. and Kasman, S. (2013) Effect of Welding Parameters on the Microstructure and Strength of Friction Stir Weld Joints in Twin Roll Cast EN AW Al-Mn1Cu Plates,*Journal of Materials Engineering and Performance* 22(10), 3024-3033.

[8] Mao, Y., Ke, L., Liu, F., Huang, C., Chen, Y. and Liu, Q. (2015) Effect of welding parameters on microstructure and mechanical properties of friction stir welded joints of 2060 aluminum lithium alloy,*The International Journal of Advanced Manufacturing Technology* 81(5), 1419-1431.

[9] DeRose, J., Balkowiec, A., Michalski, J., Suter, T., Kurzydlowski, K. and Schmutz, P. (2013) Microscopic and macroscopic characterisation of an aerospace aluminium alloy (AA2024) In: DeRose, J., Suter, T., Hack, T., Adey, R.A. (Eds) *Aluminium alloy corrosion of aircraft structures: Modelling and simulation*, Billerica, WIT Press, 23-38.

[10] Lin, Y. C., Xia, Y.-C., Jiang, Y.-Q., Zhou, H.-M. and Li, L.-T. (2013) Precipitation hardening of 2024-T3 aluminum alloy during creep aging,*Materials Science and Engineering: A* 565, 420-429.

[11] Zhou, J., Xu, S., Huang, S., Meng, X., Sheng, J., Zhang, H., Li, J., Sun, Y., Boateng, E.A. (2016), Tensile Properties and Microstructures of a 2024-T351 Aluminum Alloy Subjected to Cryogenic Treatment,*Metals* 6(11), 10.

[12] Radutoiu, N., Alexis, J., Lacroix, L., Abrudeanu, M. and Petit, J. A. (2013), Study of the Influence of the Artificial Ageing Temperature on the AA2024 Alloy Microstructure,*Key Engineering Materials* 550, 115-125.

[13] Hasan, M. M., Ishak, M. and Rejab, M. R. M. (2017), Effect of backing material and clamping system on the tensile strength of dissimilar AA7075-AA2024 friction stir welds,*The International Journal of Advanced Manufacturing Technology* 91(9), 3991-4007.

[14] Yuqing, M., Liming, K., Fencheng, L., Yuhua, C. and Li, X. (2016) Investigations on temperature distribution, microstructure evolution, and property variations along thickness in friction stir welded joints for thick AA7075-T6 plates,*The International Journal of Advanced Manufacturing Technology* 86(1), 141-154.

[15] Kasman, Ş. and Ozan, S. (2018). Sürtünme karıştırma kaynağı ile birleştirilmiş bağlantılarda pim çakışmasının mekanik özellikler üzerine etkisi. Ömer Halisdemir Üniversitesi Mühendislik Bilimleri Dergisi 7(2), 917-928. [Effect of pin overlap on mechanical properties of friction stir welded joints. *Nigde Omer Halisdemir University Journal of Engineering Sciences* 7(2), 917-928].

[16] Kasman, Ş. and Ozan, S. (2019), Effects of overlapping formed via pin-offsetting on friction stir weldability of AA7075-T651 aluminum alloy,*Journal of Mechanical Science and Technology* 33(2), 819-828.

[17] Kasman, Ş. and Ozan, S. (2019), Effect of pin offset on the mechanical properties of friction stir welded AA 6013 aluminum alloy plates,*Materialwissenschaft und Werkstofftechnik* 50(12), 1511-1524.

[18] Kasman, Ş. and Ozan, S. (2019) AA7075/AA6013 alaşım çiftinin sürtünme karıştırma kaynağı ile birleştirilmesinde pim çakışmasının mekanik özellikler üzerine etkilerinin incelenmesi. Ömer Halisdemir Üniversitesi Mühendislik Bilimleri Dergisi 8(1), 436-446. [Investigation of the effects of pin overlap phenomenon on the mechanical properties of friction stir welded AA7075/AA6013 alloy couple,*Nigde Omer Halisdemir University Journal of Engineering Sciences* 8(1), 436-446].

[19] Kasman, Ş. (2019), Identification of the pin offset effect on the friction stir welding (FSW) via Taguchi – Grey relational analysis: A Case study for AA 7075 – AA 6013 alloys,*Materialwissenschaft und Werkstofftechnik* 50(11), 1364-1381.

[20] ASTM E8 / E8M-16ae1, Standard Test Methods for Tension Testing of Metallic Materials, ASTM International, West Conshohocken, PA, 2016, www.astm.org.

[21] ASTM E112-13, Standard Test Methods for Determining Average Grain Size, ASTM International, West Conshohocken, PA, 2013, www.astm.org.

[22] Hao, H. L., Ni, D. R., Huang, H., Wang, D., Xiao, B. L., Nie, Z. R. and Ma, Z. Y. (2013), Effect of welding parameters on microstructure and mechanical properties of friction stir welded Al–Mg–Er alloy,*Materials Science and Engineering: A* 559, 889-896.

[23] Gharbi, O., Jiang, D., Feenstra, D., Kairy, S., Wu, Y., Hutchinson, C. and Birbilis, N. (2018), Microstructure and corrosion properties of additively manufactured aluminium alloy AA2024, In: *The proceedings of the 16th international aluminum alloys conference (ICAA16)*, Montreal.

[24] Badini, C., Marino, F. and Verné, E. (1995), Calorimetric study on precipitation path in 2024 alloy and its SiC composite,*Materials Science and Engineering: A* 191(1), 185-191.

[25] Dong, J.-h., Gao, C., Lu, Y., Han, J., Jiao, X.-d. and Zhu, Z.-x. (2017), Microstructural characteristics and mechanical properties of bobbin-tool friction stir welded 2024–T3 aluminum alloy,*International Journal of Minerals, Metallurgy, and Materials* 24(2), 171-178.

[26] Kasman, Ş. and Ozan, S. (2020) AA 2024-T351 Alüminyum Alaşımının Sürtünme Karıştırma Kaynağı ile Birleştirilmesinde Pim Kaydırmasının Mekanik Özellikler Üzerine Etkilerinin İncelenmesi, 3. Uluslararası Erciyes Bilimsel Araştırmalar Kongresi, 33, 9 Mayıs 2020, Kayseri, Türkiye.[Kasman, Ş. and Ozan, S. (2020) Investigation of the Effects of Pin Offset Phenomenon on the Mechanical Properties of Friction Stir Welded AA 2024-T351 Alloy, 3rd International Erciyes Conference on Scientific Research, 33, 9 May 2020, Kayseri, Turkey].